

1 **Title:** Machine learning reveals the effect of leaf temperature extremes on shifts in plant
2 photosystem heat tolerance thresholds

3

4 **Author names:** Catherine Pottinger¹, Pieter A. Arnold², Michelle Bird¹, Lisa M. Danzey¹,
5 Sonya R. Geange^{3,4}, Andrei Herdean⁵, Adrienne B. Nicotra², Andy Leigh¹

6 **Affiliations:**

7 ¹University of Technology Sydney, School of Life Sciences, Broadway, NSW 2007, Australia.

8 ² Division of Ecology and Evolution, Research School of Biology, The Australian National
9 University, Canberra, ACT 2600 Australia.

10 ³University of Bergen, Department of Biological Sciences, Bergen, 5008 Norway.

11 ⁴Bjerknes Centre for Climate Research, University of Bergen, Norway

12 ⁵University of Technology Sydney, Climate Change Cluster, Broadway, NSW 2007, Australia.

13

14 Catherine Pottinger: <https://orcid.org/0009-0001-2436-5069>

15 Pieter Arnold: <https://orcid.org/0000-0002-6158-7752>

16 Lisa Danzey: <https://orcid.org/0009-0005-0314-9075>

17 Sonya Geange: <https://orcid.org/0000-0001-5344-7234>

18 Andrei Herdean: <https://orcid.org/0000-0003-2143-0213>

19 Adrienne Nicotra: <https://orcid.org/0000-0001-6578-369X>

20 Andy Leigh: <https://orcid.org/0000-0003-3568-2606>

21 **Funding**

22 Australian Research Council Linkage Projects grant LP180100942, held by AN and AL;
23 Australian Government Research Training Program Scholarship, held by CP.

24 **Conflicts of Interest**

25 The authors declare no conflicts of interest.

26 **Data availability**

27 If accepted for publication, data will be made available on Dryad and the code used for
28 analyses, on GitHub.

29 **Keywords**

30 Heat tolerance, leaf temperature, microclimate, alpine, T_{crit} , cross tolerance, extreme
31 temperatures

32 **Abstract**

33 Plant physiological heat tolerance thresholds can acclimate rapidly in response to changing
34 leaf temperature, which varies considerably across microclimatic space and time. How leaf
35 temperatures trigger shifts in these heat thresholds has not been established. We aimed to
36 determine the influence of temporally proximal leaf temperatures (T^{leaf}) on leaf photosystem
37 heat tolerance thresholds (T_{crit}) for two co-occurring plant species *in situ* in the Australian
38 Alps. We measured T_{crit} and T^{leaf} over five days at 16 sites, paired by aspect (northwest,
39 southeast) across two locations: a cold air drainage valley and a high exposed ridgeline. To
40 investigate how T_{crit} was influenced by T^{leaf} in the days prior, we used traditional statistical
41 approaches (linear mixed models) and a machine learning technique. While traditional
42 models found that T^{leaf} parameters explained some variation in T_{crit} , machine learning
43 identified that 85% of the variation in T_{crit} was explained by both maximum and minimum
44 leaf temperatures in the four days prior to measurement. This finding illustrates that heat
45 tolerance acclimation is driven by exposure to not only maximum, but also minimum leaf
46 temperatures. To uncover complex relationships between fluctuating environmental
47 conditions and plant acclimatory responses, we recommend integrating machine learning
48 techniques with traditional statistical methods.

49

50 **Introduction**

51 Many of the critical physiological processes of plants, including photosynthesis, tissue repair
52 and reproduction, are mediated by temperature (Wahid et al. 2007). Ascertaining the
53 thermal limits to physiological function, or thermal tolerance thresholds, and how they shift
54 with local temperature, is critical if plant vulnerability to climatic warming is to be
55 characterised accurately (Cook et al. 2021). It is becoming increasingly clear that coarse
56 gradient measures of climate do not predict significant variation in heat tolerance thresholds
57 at a local scale (Curtis et al. 2016, Feeley et al. 2020, Perez and Feeley 2020, Danzey et al.
58 2024). Indeed, in common garden settings, differences in heat tolerance thresholds are
59 reduced relative to *in situ* measurements (Knight and Ackerly 2002, Knight and Ackerly 2003,
60 Harris et al. 2024, Alvarez et al. 2025), indicating acclimation to local conditions. Heat
61 tolerance acclimation in plants broadly refers to the reversible physiological and
62 morphological adjustments that enable plants to modify their thermal limits in according to
63 prevailing environmental conditions (Wahid et al. 2007, Zhu et al. 2018). Further, leaf
64 temperatures can strongly decouple from air, exceeding air temperatures by $>10^{\circ}\text{C}$ under
65 hot conditions (Körner and Cochrane 1983, Blonder and Michaletz 2018, Fauset et al. 2018);
66 the extent of this decoupling is mediated by morphological traits that influence leaf
67 thermodynamics (Leigh et al. 2017, Arnold et al. 2025a). For these reasons, focus has shifted
68 toward the influence of leaf temperature on thermal tolerance, particularly photosystem
69 heat tolerance (Perez and Feeley 2020, Cook et al. 2021, Zhu et al. 2024). There is evidence
70 to suggest that microclimate, through its influence on leaf temperatures, is a strong
71 predictor of heat tolerance thresholds (Buchner and Neuner 2003, Curtis et al. 2016, Leon-
72 Garcia and Lasso 2019). This association is particularly important to investigate in places
73 typified by high microclimatic heterogeneity and temporal variability, such as alpine
74 environments (Körner 2003, Körner and Hiltbrunner 2021, Körner 2023).

75 Average temperatures do not necessarily capture the extremes to which plants are exposed.
76 Nor do they account for the influence of heat load, a function of temperature intensity and
77 exposure duration, on heat tolerance (Neuner and Buchner 2023, Cook et al. 2024, Faber et
78 al. 2024). While climate change is bringing warmer daytime temperatures, nighttime
79 temperatures may be increasing at a greater rate (Easterling et al. 1997, Donat and
80 Alexander 2012), which has implications on important aspects of plant physiology and

81 reproduction (Willits and Peet 1998, Niu and Xiang 2018, Rahnama et al. 2024). Among
82 these physiological processes, PSII acclimation is particularly important, as it reflects the
83 ability of the photosynthetic apparatus to maintain function under increasingly stressful
84 thermal conditions. This phenomenon has been observed as changes in PSII heat tolerance
85 thresholds (Posch et al. 2022, Sumner et al. 2022, Andrew et al. 2023, Cook et al. 2024,
86 Danzey et al. 2024). Research on heat tolerance thresholds typically focuses on the effect of
87 increasing or maximum temperatures (Leon-Garcia and Lasso 2019, Perez and Feeley 2020,
88 Vilas-Boas et al. 2024), while the effect of minimum temperatures has received far less
89 attention. Further, diurnal temperature amplitude can exert a substantial effect on drought
90 and freezing tolerance (Zhang et al. 2023). However, the effect of temperature across diurnal
91 cycles on heat tolerance thresholds under natural conditions remains to be studied.

92 Regarding the effect of temperature history on heat tolerance, some authors suggest that
93 acclimation is influenced by mean and maximum daily temperatures in the days prior to
94 measurement (Hüve et al. 2006, Curtis 2017, Bison and Michaletz 2024, Zhu et al. 2024).
95 Conversely, others have found that acclimation of heat thresholds occurs over longer
96 temporal scales, across months and seasons (Zhu et al. 2018, Leon-Garcia and Lasso 2019).
97 It remains unclear as to what temporal scale acclimation of these thresholds occurs across
98 and the magnitude of the cues that trigger threshold shifts.

99 The thermal triggers for heat tolerance acclimation are complex. Relationships between
100 heat tolerance and temperature are not linear, with discrepancies between threshold
101 relaxation and leaf temperature documented in alpine environments (Buchner and Neuner
102 2003, Neuner and Buchner 2012). Therefore, traditional statistical methods that rely on
103 average temperatures to predict heat tolerance present clear limitations, particularly for
104 data collected under field conditions, where environmental temperatures vary across
105 microclimates and plants are exposed to rapid temperature fluctuations. Predicting thermal
106 tolerance necessitates a more nuanced assessment of how temporally proximal
107 temperatures lead to shifts in heat tolerance thresholds. Machine learning has recently
108 been used to determine how leaf temperature series predict plant physiological processes
109 like stomatal conductance (Gaur and Drewry 2024). Others have used such methods for
110 predicting photosynthetic performance parameters from plant water status and spectral
111 characteristics (Yang et al. 2022, Song and Wang 2023). A machine learning approach offers

112 a potential path for ascertaining how leaf temperature profiles might cue changes in heat
113 tolerance thresholds.

114 Here we measured *in situ* leaf and air temperatures and critical heat tolerance thresholds of
115 photosystem II (PSII) of two co-occurring morphologically and phylogenetically distinct
116 Australian alpine plant species, *Grevillea australis* and *Dracophyllum continentis*, at 16 sites
117 across two locations varying in elevation and landform. By contrasting the aspect and
118 location of study sites, our design maximised the microclimatic variation in terms of the
119 average time of day that maximum temperature occurred, the sum of temperatures across a
120 day and the temperature range of the diurnal cycle. We compared two different approaches
121 to investigate how leaf temperature affects acclimation of plant heat tolerance thresholds.

122 First, representing a traditional statistical approach, we used linear mixed models to
123 determine whether average temperature parameters could explain variations in heat
124 tolerance thresholds. Second, we sought to explain variation in T_{crit} by applying a machine
125 learning (ML) approach, which used the full suite of raw temperature data, representing
126 5,600 individual leaf temperature points.

127 **Methods**

128 *Study site selection and study species*

129 All field and experimental work was conducted on Wolgalu and Monaro Ngarigo lands in
130 Kosciuszko National Park, New South Wales, Australia. Study sites were situated in
131 grasslands at two locations representing different topographies and elevations: Schlink Pass,
132 a sub-alpine, cold air drainage valley along the Munyang River, at 1670 m a.s.l., and Mt
133 Stilwell, an alpine site on the exposed mountain pass above Charlotte Pass Village, 1959 m
134 a.s.l. Aspect, topography and elevation are design features that influence microclimatic
135 conditions. There were 16 sites in total: at each location, eight sites were selected, four of
136 NW aspect and four of SE aspect (Figure 1a; Figure S1; Table S1). Along with the contrasting
137 landforms represented at the two locations, selecting sites with contrasting aspects
138 maximised potential microclimatic variation, based on two factors: first, prevailing winds in
139 the region are from the west to the northwest (AGBoM 2023) and second, incident sunlight
140 is highest for equatorial-facing vegetation (Russell et al. 1989), i.e., north-northwest in the
141 southern hemisphere (for more details, see Supporting Information 1).

142 The two alpine species, *Dracophyllum continentis* B.L.Burtt (Ericaceae) and *Grevillea australis*
143 R.Br. (Proteaceae), are found in both alpine and subalpine environments throughout South-
144 East Australia. These species were selected because they co-occur in moist alpine
145 environments yet are phylogenetically and morphologically distinct. *Dracophyllum*
146 *continentis* is a multi-branched shrub growing to 1 m, with thick, ovate to triangular leaves
147 (2–4 cm long, 4–7 mm wide), densely packed around the stem; *G. australis* is a shrub
148 growing to 1 m, with smaller, oblanceolate, linear, or narrow-elliptic leaves (0.5–3.5 cm long,
149 0.5–5.5 mm wide) that are spread along its woody branches (PlantNET 2024).

150 *Air and leaf temperature measurements*

151 Site-specific air temperature and leaf temperatures of *G. australis* and *D. continentis* were
152 measured at all 16 sites across Schlink Pass and Mt Stilwell from the start of February 2023
153 (Figure S2a, b). Leaf temperature was logged in 5-minute intervals using fine-wire type-T
154 thermocouples (gauge AWG 36, 0.13 mm diameter, Omega Engineering, Norwalk, CT, USA)
155 connected to four-channel HOBO data loggers (UX120-014M, Onset HOBO® Dataloggers
156 Onset, Bourne, USA). At each site, one thermocouple was attached to the underside of a *D.*
157 *continentis* leaf and two were attached to *G. australis* leaves. Thermocouples were affixed to
158 the leaves using a small piece of surgical tape, sized to one third of the leaf area to minimise
159 disruption to the leaf boundary layer (Figure S2c, d). All thermocouples measuring leaf
160 temperature were attached to leaves on the outer, sun-exposed north-facing side of the
161 canopy. Another thermocouple measured ambient air temperature and was attached to a
162 branch adjacent to the leaves being measured for temperature. A small white cap covered
163 each air thermocouple to shield it from direct sunlight (Figure S2e, f).

164 *Collection of leaf material*

165 Sampling of leaves for heat tolerance thresholds took place during mid-summer, between
166 9am and 12pm every day from 26 February to 2 March 2023. To determine the water status
167 of the plants sampled for heat tolerance measurement, we also collected leaves RWC
168 between 25 February and 1 March. The field sites were logistically very challenging to access
169 on foot, so water potential measurements were not feasible. To ensure that heat tolerance
170 measurements were not confounded by time of sampling, leaves were collected from all 16
171 sites each day by two fieldwork teams concurrently, one at Mt Stilwell and the other at
172 Schlink Pass. At each site, two mature, healthy leaves were collected from the outer sun-

173 exposed north side of the canopy for each species. Concurrently, a small stem bearing leaves
174 of the same description was collected for relative water content (RWC) measurement. On
175 each day of sampling, leaves were collected from the same plants at each site. After
176 collection, leaves were placed in zip-lock bags lined with damp paper towels and kept in
177 darkness until heat tolerance measurements were made in the laboratory the same day.
178 Leaf samples were measured between five and eight hours after collection (Danzey et al.
179 2024, Briceño et al. 2025).

180 *Measurement of heat tolerance thresholds*

181 Photosystem II heat tolerance thresholds were measured based on the method detailed by
182 Arnold et al. (2021). Briefly, leaf samples were placed on a thermoelectrically controlled
183 Peltier plate, with type-T thermocouples attached to the underside of each leaf sample for
184 continuous leaf temperature measurements during a controlled heating ramp. The
185 temperature ramp began at 25 °C, increasing at a rate of 0.5 °C per minute until reaching
186 70 °C. A pulse amplitude modulated imaging fluorimeter (Maxi-Imaging-PAM; Heinz Walz
187 GmbH, Effeltrich, Germany) took measurements of minimal chlorophyll fluorescence (F_0)
188 during heating after allowing 30 minutes for leaves to dark adapt. For each experimental
189 run, 64 T- F_0 curves (two replicates from the 16 sites for each species) were produced, from
190 which the critical heat thresholds (T_{crit}) were determined as the point of transition between
191 slow-rise and fast-rise in F_0 with increasing temperature (Figure S3).

192 *Meausrement of RWC*

193 For relative water content (RWC) determination, leaf samples with petioles removed were
194 first weighed to obtain fresh weight (FW). Samples were then submerged in water-filled pill
195 boxes for 3–4 hours to allow rehydration, after which the turgid weight (TW) was recorded.
196 Subsequently, samples were transported to the laboratory and oven-dried for one week,
197 after which they were re-weighed to obtain the dry weight (DW). RWC was calculated using
198 the formula:

$$199 \quad RWC = \frac{FW - DW}{TW - DW} \times 100$$

200 *Traditional statistical approach for ascertaining the effect of leaf temperature on T_{crit}*

201 To characterise microclimatic variation in thermal profile across study sites, we calculated
202 three temperature parameters that we expected to reflect the nature, intensity and timing
203 of thermal load to which plants are exposed. These factors have been shown to influence
204 plant heat tolerance (Blair et al. 2019, Grinevich et al. 2019, Laosuntisuk and Doherty 2022,
205 Neuner and Buchner 2023, Cook et al. 2024). Heat stress intensity varies with aspect as it
206 determines the timing and magnitude of maximum temperatures in each day (McCune and
207 Keon 2002, Li et al. 2021). Thermal regimes differ markedly between mountain and valley
208 environments. While air temperatures are typically higher in lower elevation environments
209 at night, radiative cooling and cold-air drainage promote the formation of cold air pools,
210 which tend to develop in valleys (Lundquist et al. 2008, Pepin et al. 2022). As such, we chose
211 to calculate the time of day that maximum air temperature was reached (T_{time}^{air}), the daily
212 sum of degrees above 0°C (T_{sum}^{air}), and the diurnal cycle temperature range (T_{range}^{air}) at each
213 of the 16 study sites for the four weeks prior to and coinciding with T_{crit} measurement (Table
214 S2).

215 First, the temperature data for each site were cleaned to remove non-sensible values due to
216 spurious electrical signals (below -25°C and above 40°C). For calculation of T^{leaf} values for *G.*
217 *australis*, raw leaf temperature data collected by the two thermocouples were averaged. To
218 calculate T_{sum} values, the average temperatures above 0°C were summed for each five-
219 minute interval across the 24 hours between 12 am and 11:59 pm for each day. For T_{time} , the
220 time at which the maximum temperature occurred on each day was converted into hour
221 values for ease of analysis (e.g., a 24-hour time value of 13:30 became 13.5). T_{range}
222 parameters were calculated by subtracting the minimum temperature occurring each night
223 (between 7 pm and 6:59 am) from the maximum temperature occurring on the subsequent
224 day (between 7 am and 6:59 pm). In addition to calculating 24-hour cumulative temperature
225 above 0 °C (T_{sum}^{leaf}) on T_{crit} , nightly ($T_{sum-night}^{leaf}$) and daily temperature ($T_{sum-day}^{leaf}$) sums
226 were calculated separately so we could differentiate between the effects of day and
227 nighttime heat load on T_{crit} . $T_{sum-day}^{leaf}$ and $T_{sum-night}^{leaf}$ were calculated by summing the
228 temperatures above 0°C for each 5-minute interval between 7 am and 6:59 pm and 7 pm
229 and 6:59 am respectively. Individual daily values for each T^{air} parameter at each site were
230 averaged across all days of February, resulting in 16 levels of each microclimate parameter.
231 Values for each T^{leaf} parameter were averaged at each site and for each species across the

232 days preceding and coinciding with T_{crit} sampling (22 Feb – 28 Feb) resulting in 32 levels of
233 each leaf temperature parameter.

234 To assess whether plants from these distinct microclimates differed in water status, we fitted
235 an LMM with the same structure as above, but with RWC as the response variable and plant
236 ID included as an additional random factor and species as an additional fixed factor. While
237 RWC differed significantly between species ($F_{1, 27} = 52.9$, $p < 0.001$), it did not with location
238 ($F_{1, 27} = 0.43$, $p = 0.52$) or aspect ($F_{1, 27} = 0.0059$, $p = 0.94$; Figure S4). This analysis enabled
239 us to exclude variation in plant water status across sites as a factor potentially confounding
240 microclimatic variation in T_{crit} .

241 Having established that T_{time}^{air} , T_{sum}^{air} and T_{range}^{air} reflect the substantial microclimatic
242 variation among sites (Table S3), we next sought to determine the influence of the
243 equivalent leaf temperature versions of these parameters on heat tolerance thresholds. Leaf
244 temperature parameters (T_{time}^{leaf} , T_{sum}^{leaf} and T_{range}^{leaf}) were calculated using the measured
245 leaf temperatures of *G. australis* and *D. continentis* spanning the four days prior to, and first
246 three days of T_{crit} sampling (Figure S5), which we expected to most closely reflect the
247 temperature conditions likely to initiate changes in heat tolerance thresholds (Bison and
248 Michaletz 2024, Zhu et al. 2024). In addition to calculating 24-hour cumulative temperature
249 above 0 °C (T_{sum}^{leaf}) on T_{crit} , nightly ($T_{sum-night}^{leaf}$) and daily temperature ($T_{sum-day}^{leaf}$) sums
250 were calculated separately so we could differentiate between the effects of day and
251 nighttime heat load on T_{crit} . All temperature parameters were averaged across the seven
252 days for each of the 16 sites and the resulting values were included as fixed factors in three
253 separately fitted LMMs, where T_{crit} was the response variable. In each model, date was
254 included as a random factor to account for weather variation across sampling days. To
255 prevent boundary fit issues arising from including aspect and location separately, a
256 categorical variable named ‘site type’ with four levels (SchlinkSE, SchlinkNW, StilwellNW,
257 StilwellSE) was used as a random factor in these models. Where boundary fit issues
258 persisted, ‘site type’ was removed from the model. An additional random effect was added
259 to the models, Plant ID, of which there were 32 levels, to account for variability between leaf
260 replicates. ‘Species’ was excluded from $T^{leaf} \sim T_{crit}$ models as a fixed term because
261 preliminary analyses determined that T_{crit} did not differ between species ($F_{1, 286} = 0.087$, $p =$

262 0.77). Analyses were conducted using R Statistical Software (v 4.2.1: R Development Core
263 Team 2024).

264 *Machine learning approach to ascertaining the effect of leaf temperature on T_{crit}*

265 Boosting-based ensemble methods are a class of machine learning algorithms that combine
266 multiple decision trees into a single strong predictive model. Each decision tree is trained
267 sequentially, with each subsequent model attempting to correct the residual errors of its
268 predecessor. This learning process allows boosting models to capture complex, nonlinear
269 relationships between input, predictive features and response variables (Natekin and Knoll
270 2013). We utilised the IBM Watson Machine Learning platform to train a Snap Boosting
271 Machine Regressor model to identify key predictive temperature points leading up to T_{crit}
272 measurements. For the machine learning model (Python script) see Supplementary File 1.
273 Five-minute interval leaf temperature data from both species and all sites were pooled
274 together for training the model. This pooled model resulted in 153 T_{crit} values with their
275 respective temperature history, which initially encompassed 25 days prior to each T_{crit}
276 measurement (1 February 2023 – 1 March 2023; 8,532 time points and 267,264 leaf
277 temperature points for each day of T_{crit} measurement for the initial 29-day model). Based on
278 this preliminary analysis, we narrowed this down to the four-day temperature history
279 leading up to each T_{crit} measurement (1,152 time points and 36,864 leaf temperatures points
280 for each day of T_{crit} measurement, Figure S6), as it provided the most relevant predictive
281 features. This decision was supported by literature on the biochemical processes that govern
282 heat tolerance; for example, decay of upregulated heat shock proteins has been shown to
283 occur between 2 and 3 days after heat stress (Charng et al. 2006, Aspinwall et al. 2019).
284 These findings align with the three days prior to T_{crit} measurement being the best predictive
285 window for shifts in heat tolerance (Bison and Michaletz 2024, Zhu et al. 2024).

286 **Results**

287 *T^{leaf} parameters appear to predict little variation in T_{crit}*

288 Three leaf temperature parameters (T_{time}^{leaf} , T_{sum}^{leaf} and T_{range}^{leaf}) were included as fixed
289 factors in separate LMMs where T_{crit} was the response variable (Table 2). Accounting for site
290 type (location-aspect combination: SchlinkNW, SchlinkSE, StilwellNW, StilwellISE), T_{sum}^{leaf}
291 predicted significant variation in T_{crit} , such that for a 313.5°C increase in T_{sum}^{leaf} , T_{crit} increased

292 by 1°C (Table 2, Figure 2b). No significant relationship of $T_{\text{time}}^{\text{leaf}}$, $T_{\text{sum-day}}^{\text{leaf}}$, $T_{\text{sum-night}}^{\text{leaf}}$
293 $T_{\text{range}}^{\text{leaf}}$ with T_{crit} was found (Table 2, Figure 2c, d; Figure S7; Table S4). The reason that the
294 positive $T_{\text{sum}}^{\text{leaf}} \sim T_{\text{crit}}$ relationship was relatively weak might be attributed to the nature of
295 the variation in T_{crit} across sampling days. Although date was a strong predictor of variation
296 in T_{crit} , the only day where T_{crit} was significantly different from the rest was on 28 Feb. T_{crit}
297 values were on average $2.8 \pm 0.9^\circ\text{C}$ higher on 28 Feb than the rest but across all other days,
298 T_{crit} values were relatively uniform (Figure 2a). To assess whether these elevated 28 February
299 values were driving the significant $T_{\text{sum}}^{\text{leaf}} \sim T_{\text{crit}}$ relationship, we re-ran the model with these
300 values excluded. The relationship was no longer significant, indicating that the 28 February
301 T_{crit} values were indeed responsible for the original significance.

302 *Machine learning reveals that preceding high and low temperatures can predict T_{crit}*
303 The machine learning results highlighted specific temperatures and times within the
304 temperature histories that were critical for predicting T_{crit} (coloured circles, Figure 3a). A
305 total of 33 leaf temperature time points within the four-day temperature window, which
306 were common to all leaves, were identified as collectively contributing 84.9% of the model's
307 total predictive power. The identified times points were predominantly high and low leaf
308 temperature values within the four-day period preceding T_{crit} measurement. The strength of
309 predictive power was distributed relatively uniformly across the 4-day period. Three leaf
310 temperature points, however, one maximum and two minima occurring between 81 and 45
311 h prior to T_{crit} measurement, provided 36.8% of the total predictive power (grey ellipses,
312 Figure 3b).

313 **Discussion**

314 The current study sought to determine how spatially and temporally varying leaf
315 temperatures drive changes in T_{crit} photosystem heat thresholds using two distinct
316 approaches: linear mixed models (LMMs) and machine learning (ML). Specifically, we were
317 interested in the insights that each method could provide about the role of prior leaf
318 temperature history in determining these thresholds, a question that has been explored
319 little to date. Temperature regimes show considerable spatial variation in alpine
320 environments, especially as a function of elevation and aspect (Legates and Willmott 1990,
321 McCune and Keon 2002). In our study, microclimatic variation with aspect and elevation was

322 characterised by different times of day that maximum air temperatures were reached, the
323 sum or load of temperature and the diurnal cycle temperature range. However, LMMs
324 revealed that the only corresponding leaf temperature parameter that predicted variation in
325 photosystem heat thresholds was average daily heat sum ($T_{\text{sum}}^{\text{leaf}}$) and that relationship was
326 weak. Whereas leaf temperature parameters were not compelling predictors of T_{crit} based
327 on LMMs, the novel ML approach was able to account for the complexity of the entire
328 thermal profile. Machine learning revealed that leaf temperature extremes, both high and
329 low, within the four days preceding heat tolerance measurements explained nearly 85% of
330 the variation in T_{crit} .

331 *Increases in mean daily heat load weakly correlates with increases in T_{crit}*

332 Mounting evidence suggests that photosystem heat tolerance thresholds respond to local
333 thermal conditions, varying temporally (Neuner et al. 2000, Coast et al. 2022, Posch et al.
334 2022) and spatially (Curtis et al. 2016, O'Sullivan et al. 2017, Cook et al. 2021, Danzey et al.
335 2024, Kullberg and Feeley 2024). While averages of point leaf temperature measurements
336 are typically used to characterise the conditions to which a plant is exposed, these metrics
337 do not capture the complex range of thermal conditions, nor the cumulative nature of heat
338 stress, which have important implications on measuring shifts in physiological tolerance
339 (Neuner and Buchner 2023, Cook et al. 2024, Faber et al. 2024). The weak $T_{\text{sum}}^{\text{leaf}} \sim T_{\text{crit}}$
340 relationship was driven by high T_{crit} values on 28 Feb. This relationship may have been
341 weakened due to the relatively benign leaf temperatures in the week leading up to T_{crit}
342 measurement (22.5°C on average). Interestingly, no significant relationship of $T_{\text{sum-day}}^{\text{leaf}}$ or
343 $T_{\text{sum-night}}^{\text{leaf}}$ with T_{crit} was observed. This finding suggests that thermal tolerance cannot be
344 understood by examining daytime or nighttime conditions in isolation. Given that sites
345 clearly had different microclimatic profiles through time, these findings suggest that LMM
346 analytical approaches that average across substantial daily leaf temperature variation
347 obscure biologically important information.

348 *Machine learning reveals preceding temperature extremes that predict shifts in T_{crit}*

349 Using machine learning, we found compelling evidence that certain daily leaf temperature
350 points prior to measurement predict subsequent shifts in T_{crit} . The extremes of daily
351 maximum and, importantly, nightly minimum temperatures up to four days prior to heat
352 threshold measurement predicted a combined 85% of the variation in T_{crit} . The field of

353 cross-tolerance, where exposure to one kind of stress results in tolerance to another
354 (Hossain et al. 2018), may explain this potentially counterintuitive pattern. Harris et al.
355 (2024) found that the occurrence of a hot day in concert with a cold night increases heat
356 tolerance more than a hot day and warm night, suggesting that exposure to cold stress
357 improves tolerance to heat stress. Indeed, both types of thermal stress can activate similar
358 response pathways (Mei and Song 2010, Li et al. 2014, Hossain et al. 2018). Heat shock
359 proteins (HSPs) are known to upregulate in response to both heat and cold stress (Anderson
360 et al. 1994, Wang et al. 2003), with small HSPs (common in plant chloroplasts) detectable
361 for up to 72 h after a triggering event (Charng et al. 2006). Further, there is evidence to
362 suggest that increases in reactive oxygen species and subsequent upregulation of
363 antioxidant enzymes are involved in the deployment of cross-tolerance (Gong et al. 2001,
364 Hossain et al. 2016, Hossain et al. 2018).

365 In the current study, lower nightly temperatures followed by higher daily temperatures
366 might have had an acclimatory effect on heat tolerance by activating similar response
367 pathways, which manifested as increased T_{crit} in the days following. Danzey et al. (2024)
368 found PSII cold tolerance thresholds of -10.8°C for *G. australis* and -10.3°C for *D.*
369 *continentis*. In our study, the average of nightly leaf temperatures across the 7-day window
370 preceding T_{crit} measurements were -2.8°C and -3.3°C for *G. australis* and *D. continentis*,
371 respectively, with leaf temperatures dropping as low as -6.9°C across this period. While
372 these temperatures did not surpass the reported cold tolerance thresholds, they
373 approached this range. Repeated exposure to near cold thresholds likely contributed to the
374 observed acclimation. Conversely, maximum temperatures approached heat tolerance
375 thresholds measured in the current study much less closely; average maximum leaf
376 temperature across sites and both species was $22.5 \pm 0.26^{\circ}\text{C}$, while average T_{crit} was $47.8 \pm$
377 0.2°C . Such disparities between maximum temperatures and temperature thresholds have
378 been observed by others, particularly in cooler climate species (Buchner and Neuner 2003,
379 Kitudom et al. 2022, Cox et al. 2025). The stress induced by consistent low-grade stress can
380 equate to that incurred by short, intense temperature stress (Neuner and Buchner 2023,
381 Cook et al. 2024, Arnold et al. 2025b). In the context of the present study, it is plausible that
382 the moderate maximum leaf temperatures observed maintained relatively high baseline T_{crit}
383 values. Further, plants from environments with high seasonal or interannual variability may

384 maintain elevated T_{crit} as a buffer against rare but damaging extremes. Although our 5-min
385 averages showed mid-20 °C maxima, brief spikes (e.g., 30–35 °C) may have been missed yet
386 sufficient to induce acclimation, especially because induction temperatures can lie well
387 below damage thresholds (Knight and Ackerly 2002). As well as prior exposure to heat
388 stress, increased heat tolerance in plants can be induced by priming with other abiotic
389 stressors, such as drought exposure can also enhance heat tolerance (Ru et al. 2022, Sumner
390 et al. 2022, Yadav et al. 2022, Kamran et al. 2025). In this study, drought stress was unlikely
391 to be a confounding factor because relative water content remained consistent across site
392 types (Figure S4) and rarely declined to levels indicative of water stress during the sampling
393 period. An alternative explanation for why both maximum and minimum leaf temperature
394 predict heat threshold shifts is rapid acclimation and subsequent de-acclimation, which
395 frequently occur in thermally fluctuating alpine environments (Buchner and Neuner 2003).
396 Rapid acclimatory responses maybe associated with diurnal alterations of sugar
397 concentrations and osmotic potential (Seemann et al. 1986, Meyer and Santarius 1998,
398 Coast et al. 2022). Average daily maximum temperatures in alpine environments may not
399 seem stressful in absolute terms, but a sufficiently large diurnal swing between minima and
400 maxima could be. In our study, leaf temperature maxima in the days prior to T_{crit}
401 measurements might have primed leaves for subsequent high temperatures, such that a
402 cold night followed by another hot day would lead to an acclimatory shift in T_{crit} . Plants may
403 have de-acclimated when exposed to lower day time temperatures on 26 February (Figure
404 S5). When temperatures rose on 27–28 February, plants likely re-acclimated, reflected in the
405 higher T_{crit} measured on 28 February. This sequence of de-acclimation and subsequent re-
406 acclimation over 27–28 February likely drove the significant $T_{sum} \sim T_{crit}$ relationship.
407 Acclimation of T_{crit} within a three-day window has recently been observed by others (Bison
408 and Michaletz 2024), perhaps underpinned by upregulation of HSPs and changes in
409 membrane fatty acid composition (Zhu et al. 2024) and/or by expression of genes or
410 isoforms associated with photosynthesis and solute transport (Roces et al. 2022). Because
411 the ability of machine learning to identify lag effects of temperature fluctuations on T_{crit} is
412 not predicated on linear relationships, the approach is well-suited for capturing these
413 complex acclimation dynamics, especially in field conditions, where environmental
414 conditions fluctuate frequently.

415 Irrespective of how these extreme temperatures triggered shifts in heat tolerance, the same
416 response was evident for both species. No differences in the predictive points were seen
417 between species when separate machine-learning analyses were performed for them
418 (results not shown). Likewise, when testing for the main effects of species using linear mixed
419 models, no significant effect of species on T_{crit} was found. Growth form and leaf traits,
420 including but not limited to, leaf angle, leaf mass per area and leaf habit have been reported
421 as being significant predictors of heat tolerance (Sklenář et al. 2016, Sastry and Barua 2017,
422 Leon-Garcia and Lasso 2019, Middleby et al. 2025). Further, transpiration rates influence
423 leaf energy balance and perhaps heat tolerance thresholds (Marchin et al. 2022, Valliere et
424 al. 2023). It is, therefore, possible that because *G. australis* and *D. continentis* are both
425 evergreen alpine shrubs of similar heights, differences in leaf temperature driven by leaf
426 structural traits or transpiration (Bird et al. unpublished data) might not have been great
427 enough to cause differences in T_{crit} . We note, however, our restriction to just two species
428 limits the ability to draw general conclusions about different species responses, something
429 that warrants further research.

430 *Conclusions and future directions*

431 Our findings indicate that not only temporally proximal leaf temperature maxima, but also
432 minima play a significant role in triggering shifts in heat tolerance thresholds. Our study also
433 corroborated the importance of cumulative heat load in determining heat tolerance
434 thresholds. However, this direct cumulative effect was small, highlighting that average leaf
435 temperature parameters do not sufficiently capture the temporal variability in thermal
436 conditions that influence physiological tolerance thresholds. By contrast, machine learning
437 revealed patterns that traditional statistical methods could not, providing new insights into
438 acclimatory triggers for shifts in thermal tolerance threshold. The observation that both high
439 and low temperature extremes are important predictors of T_{crit} underscores the importance
440 of considering both ends of the temperature spectrum when predicting plant responses to
441 heat stress. Future studies should investigate whether cross tolerance represents a
442 competitive advantage for species from thermally variable environments. With a larger
443 sample size and broader range of species, machine learning may reveal the requirements for
444 thermal cues to induce cross-tolerance responses. Additionally, such an approach may clarify

445 whether acclimation to temperatures in the four days preceding threshold measurement is a
446 consistent and generalisable phenomenon.

447 In summary, while statistical approaches are useful for understanding broad ecological
448 patterns, machine learning could be particularly useful when dealing with spatially and
449 temporally fluctuating environmental conditions and where their relationships with plant
450 physiology are complex and non-linear. Combining machine learning with more traditional
451 statistical approaches could enhance predictive accuracy, enabling the development of
452 robust tools to guide ecosystem management, conservation strategies, and climate
453 resilience efforts.

454 **Author contributions**

455 CP, AL, PA, SG, AN, AH and LD conceived of and designed the project; CP, MB and LD
456 conducted site selection and field work; CP conducted physiological measurements; CP, LD,
457 PA and AH carried out data analyses; CP and AL lead the writing; all authors contributed to
458 writing.

459 **Acknowledgements**

460 This work was conducted on the traditional lands and waters of the Ngarigo, Walgalu,
461 Ngunnawal, Ngambri and Gadigal; we acknowledge their Elders, past, present and emerging.
462 We are grateful for the help of field volunteers: Lisa Danzey, Jeanette Jeffreys, Finn Billaryd-
463 Currey, Jay Nicholson, Michelle Bird and Anne Pottinger. The research was conducted in
464 association with Australian Research Council Linkage Project grant: LP180100942.

465 **References**

466 AGBoM (2023) Rose of Wind direction versus Wind speed in km/h: Charlotte Pass (Kosciusko
467 Chalet).

468 Alvarez PR, Harris RJ, Cook AM, Briceño VF, Nicotra AB, Leigh A (2025) Native Australian
469 seedlings exhibit novel strategies to acclimate to repeated heatwave events.
470 *Oecologia* 207(6): 84

471 Anderson JV, Li QB, Haskell DW, Guy CL (1994) Structural organization of the spinach
472 endoplasmic reticulum-luminal 70-kilodalton heat-shock cognate gene and
473 expression of 70-kilodalton heat-shock genes during cold acclimation. *Plant
474 Physiology* 104(4): 1359–1370

475 Andrew SC, Arnold PA, Simonsen AK, Briceño VF (2023) Consistently high heat tolerance
476 acclimation in response to a simulated heatwave across species from the broadly
477 distributed *Acacia* genus. *Functional Plant Biology* 50(1): 71–83

478 Arnold PA, Briceño VF, Gowland KM, Catling AA, Bravo LA, Nicotra AB (2021) A high-
479 throughput method for measuring critical thermal limits of leaves by chlorophyll
480 imaging fluorescence. *Functional Plant Biology* 48(6): 634–646

481 Arnold PA, White MJ, Cook AM, Leigh A, Briceño VF, Nicotra AB (2025a) Plants originating
482 from more extreme biomes have improved leaf thermoregulation. *Annals of Botany*
483 136(1): 199–213

484 Arnold PA, Noble DWA, Nicotra AB, Kearney MR, Rezende EL, Andrew SC, Briceño VF,
485 Buckley LB, Christian KA, Clusella-Trullas S, Geange SR, Guja LK, Jiménez Robles O,
486 Kefford BJ, Kellermann V, Leigh A, Marchin RM, Mokany K, Bennett JM (2025b) A
487 Framework for Modelling Thermal Load Sensitivity Across Life. *Global Change
488 Biology* 31(7): e70315

489 Aspinwall MJ, Pfautsch S, Tjoelker MG, Vårhammar A, Possell M, Drake JE, Reich PB, Tissue
490 DT, Atkin OK, Rymer PD, Dennison S, Van Sluyter SC (2019) Range size and growth
491 temperature influence Eucalyptus species responses to an experimental heatwave.
492 *Global Change Biology* 25(5): 1665–1684

493 Bird M, Pottinger C, Arnold P, Danzey L, Geange S, Kearney M, Nicotra A, Leigh A
494 (unpublished data) Can NicheMapR predict leaf temperatures of morphologically
495 disparate species across microclimatically distinct alpine sites?

496 Bison NN, Michaletz ST (2024) Variation in leaf carbon economics, energy balance, and heat
497 tolerance traits highlights differing timescales of adaptation and acclimation. *New*
498 *Phytologist* 242(5): 1919–1931

499 Blair EJ, Bonnot T, Hummel M, Hay E, Marzolino JM, Quijada IA, Nagel DH (2019)
500 Contribution of time of day and the circadian clock to the heat stress responsive
501 transcriptome in *Arabidopsis*. *Scientific Reports* 9(1): 4814

502 Blonder B, Michaletz ST (2018) A model for leaf temperature decoupling from air
503 temperature. *Agricultural and Forest Meteorology* 262: 354–360

504 Briceño VF, Arnold PA, Cook AM, Courtney Jones SK, Gallagher RV, French K, Bravo LA,
505 Nicotra AB, Leigh A (2025) Drivers of thermal tolerance breadth of plants across
506 contrasting biomes. *Journal of Ecology* in press

507 Buchner O, Neuner G (2003) Variability of heat tolerance in alpine plant species measured at
508 different altitudes. *Arctic, Antarctic, and Alpine Research* 35(4): 411–420, Article

509 Charng YY, Liu HC, Liu NY, Hsu FC, Ko SS (2006) *Arabidopsis Hsa32*, a novel heat shock
510 protein, is essential for acquired thermotolerance during long recovery after
511 acclimation. *Plant Physiology* 140(4): 1297–1305

512 Coast O, Posch BC, Rognoni BG, Bramley H, Gaju O, Mackenzie J, Pickles C, Kelly AM, Lu M,
513 Ruan Y-L, Trethowan R, Atkin OK (2022) Wheat photosystem II heat tolerance:
514 evidence for genotype-by-environment interactions. *The Plant Journal* 111(5): 1368–
515 1382

516 Cook AM, Berry N, Milner KV, Leigh A (2021) Water availability influences thermal safety
517 margins for leaves. *Functional Ecology* 35(10): 2179–2189, Article

518 Cook AM, Rezende EL, Petrou K, Leigh A (2024) Beyond a single temperature threshold:
519 Applying a cumulative thermal stress framework to plant heat tolerance. *Ecology*
520 Letters 27(3): e14416

521 Cox D, Marchin RM, Ellsworth DS, Wujeska-Klause A, Ossola A, Crous KY, Leishman MR,
522 Rymer PD, Tjoelker MG (2025) Thermal Safety Margins and Peak Leaf Temperatures
523 Predict Vulnerability of Diverse Plant Species to an Experimental Heatwave. *Plant,*
524 *Cell & Environment* in press

525 Curtis E (2017) Spatiotemporal dynamics of high-temperature tolerance in australian arid-
526 zone plants. University of Technology, Sydney,

527 Curtis EM, Gollan J, Murray BR, Leigh A (2016) Native microhabitats better predict tolerance
528 to warming than latitudinal macro-climatic variables in arid-zone plants. *Journal of*
529 *Biogeography* 43(6): 1156–1165

530 Danzey LM, Briceño VF, Cook AM, Nicotra AB, Peyre G, Rossetto M, Yap JS, Leigh A (2024)
531 Environmental and Biogeographic Drivers behind Alpine Plant Thermal Tolerance
532 and Genetic Variation. *Plants (Basel)* 13(9)

533 Donat MG, Alexander LV (2012) The shifting probability distribution of global daytime and
534 night-time temperatures. *Geophysical Research Letters* 39(14): e14707

535 Easterling DR, Horton B, Jones PD, Peterson TC, Karl TR, Parker DE, Salinger MJ, Razuvayev
536 V, Plummer N, Jamason P, Folland CK (1997) Maximum and Minimum Temperature
537 Trends for the Globe. *Science* 277(5324): 364–367

538 Faber A, Ørsted M, Ehlers K (2024) Application of the thermal death time model in
539 predicting thermal damage accumulation in plants. *Journal of Experimental Botany*
540 75(11): 3467–3482

541 Fauset S, Freitas HC, Galbraith DR, Sullivan MJP, Aidar MPM, Joly CA, Phillips OL, Vieira SA,
542 Gloor MU (2018) Differences in leaf thermoregulation and water use strategies
543 between three co-occurring Atlantic forest tree species. *Plant, Cell & Environment*
544 41(7): 1618–1631

545 Feeley K, Martinez-Villa J, Perez T, Silva Duque A, Triviño Gonzalez D, Duque A (2020) The
546 Thermal Tolerances, Distributions, and Performances of Tropical Montane Tree
547 Species. *Frontiers in Forests and Global Change* 3, Original Research

548 Gaur S, Drewry DT (2024) Explainable machine learning for predicting stomatal conductance
549 across multiple plant functional types. *Agricultural and Forest Meteorology* 350:
550 e109955

551 Gong M, Chen Bo, Li Z-G, Guo L-H (2001) Heat-shock-induced cross adaptation to heat,
552 chilling, drought and salt stress in maize seedlings and involvement of H2O2. *Journal
553 of Plant Physiology* 158(9): 1125–1130

554 Grinevich D, Stroup K, Duan J, Slabaugh E, Doherty C (2019) Novel transcriptional responses
555 to heat revealed by turning up the heat at night. *Plant Molecular Biology* 101(1): 1–
556 19

557 Harris RJ, Alvarez PR, Bryant C, Briceño VF, Cook AM, Leigh A, Nicotra AB (2024) Acclimation
558 of thermal tolerance in juvenile plants from three biomes is suppressed when
559 extremes co-occur. *Conservation Physiology* 12(1): coae027

560 Hossain MA, Burritt DJ, Fujita M (2016) Cross-Stress Tolerance in Plants: Molecular
561 Mechanisms and Possible Involvement of Reactive Oxygen Species and
562 Methylglyoxal Detoxification Systems. pp 327–380

563 Hossain MA, Li Z-G, Hoque TS, Burritt DJ, Fujita M, Munné-Bosch S (2018) Heat or cold
564 priming-induced cross-tolerance to abiotic stresses in plants: key regulators and
565 possible mechanisms. *Protoplasma* 255(1): 399–412

566 Hüve K, Bichele I, Tobias M, Niinemets U (2006) Heat sensitivity of photosynthetic electron
567 transport varies during the day due to changes in sugars and osmotic potential. *Plant
568 Cell & Environment* 29(2): 212–228

569 Kamran M, Burdiak P, Karpiński S (2025) Crosstalk Between Abiotic and Biotic Stresses
570 Responses and the Role of Chloroplast Retrograde Signaling in the Cross-Tolerance
571 Phenomena in Plants. *Cells* 14(3): 176

572 Kitudom N, Fauset S, Zhou Y, Fan Z, Li M, He M, Zhang S, Xu K, Lin H (2022) Thermal safety
573 margins of plant leaves across biomes under a heatwave. *Science of The Total
574 Environment* 806: 150416

575 Knight C, Ackerly D (2002) An ecological and evolutionary analysis of photosynthetic
576 thermotolerance using the temperature-dependent increase in fluorescence.
577 *Oecologia* 130(4): 505–514

578 Knight CA, Ackerly DD (2003) Evolution and plasticity of photosynthetic thermal tolerance,
579 specific leaf area and leaf size: congeneric species from desert and coastal
580 environments. *New Phytologist* 160(2): 337–347

581 Körner C (2003) Alpine Plant Life: Functional Plant Ecology Of High Mountain Ecosystems.
582 Springer, Germany

583 Körner C (2023) Concepts in Alpine Plant Ecology. *Plants* 12(14): 2666

584 Körner C, Cochrane P (1983) Influence of plant physiognomy on leaf temperature on clear
585 midsummer days in the Snowy Mountains, south-eastern Australia. *Acta Oecologia*
586 4: 117–124

587 Körner C, Hiltbrunner E (2021) Why is the alpine flora comparatively robust against climatic
588 warming? *Diversity* 13(8): 383

589 Kullberg AT, Feeley KJ (2024) Seasonal acclimation of photosynthetic thermal tolerances
590 in six woody tropical species along a thermal gradient. *Functional Ecology* 38(11):
591 2493–2505

592 Laosuntisuk K, Doherty CJ (2022) The intersection between circadian and heat-responsive
593 regulatory networks controls plant responses to increasing temperatures. *Biochem
594 Soc Trans* 50(3): 1151–1165

595 Legates DR, Willmott CJ (1990) Mean seasonal and spatial variability in global surface air
596 temperature. vol 41.

597 Leigh A, Sevanto S, Close JD, Nicotra AB (2017) The influence of leaf size and shape on leaf
598 thermal dynamics: does theory hold up under natural conditions? *Plant, Cell &
599 Environment* 40(2): 237–248

600 Leon-Garcia IV, Lasso E (2019) High heat tolerance in plants from the Andean highlands:
601 Implications for paramos in a warmer world. *PLoS One* 14(11): e0224218

602 Li S-L, Xia Y-Z, Liu J, Shi X-D, Sun Z-Q (2014) Effects of cold-shock on tomato seedlings under
603 high temperature stress. *The Journal of Applied Ecology* 25: 2927–2934

604 Li Xe, Song X, Zhao J, Lu H, Qian C, Zhao X (2021) Shifts and plasticity of plant leaf mass per
605 area and leaf size among slope aspects in a subalpine meadow. *Ecology and
606 Evolution* 11(20): 14042–14055

607 Lundquist JD, Pepin N, Rochford C (2008) Automated algorithm for mapping regions of cold-
608 air pooling in complex terrain. *Journal of Geophysical Research: Atmospheres*
609 113(D22)

610 Marchin RM, Backes D, Ossola A, Leishman MR, Tjoelker MG, Ellsworth DS (2022) Extreme
611 heat increases stomatal conductance and drought-induced mortality risk in
612 vulnerable plant species. *Global Change Biology* 28(3): 1133–1146

613 McCune B, Keon D (2002) Equations for potential annual direct incident radiation and heat
614 load. *Journal of vegetation science* 13(4): 603–606

615 Mei YQ, Song SQ (2010) Response to temperature stress of reactive oxygen species
616 scavenging enzymes in the cross-tolerance of barley seed germination. *Journal of*
617 *Zhejiang University Science B* 11(12): 965–972

618 Meyer H, Santarius KA (1998) Short-term thermal acclimation and heat tolerance of
619 gametophytes of mosses. *Oecologia* 115(1-2): 1–8

620 Middleby KB, Cheesman AW, Hopkinson R, Baker L, Ramirez Garavito S, Breed MF, Cernusak
621 LA (2025) Ecotypic Variation in Leaf Thermoregulation and Heat Tolerance but Not
622 Thermal Safety Margins in Tropical Trees. *Plant, Cell & Environment* 48(1): 649–663

623 Natekin A, Knoll A (2013) Gradient boosting machines, a tutorial. *Front Neurorobot* 7: 21

624 Neuner G, Buchner O (2012) Dynamics of Tissue Heat Tolerance and Thermotolerance of PS
625 II in Alpine Plants. In: Lütz C (ed) *Plants in Alpine Regions: Cell Physiology of Adaption*
626 and Survival Strategies. Springer Vienna, Vienna, pp 61–74

627 Neuner G, Buchner O (2023) The dose makes the poison: The longer the heat lasts, the
628 lower the temperature for functional impairment and damage. *Environmental and*
629 *Experimental Botany* 212(4): 105395

630 Neuner G, Buchner O, Braun V (2000) Short-term changes in heat tolerance in the alpine
631 cushion plant *silene acaulis* ssp. *Excapa* [all.] j. *Braun* at different altitudes. *Plant*
632 *Biology* 2(6): 677–683

633 Niu Y, Xiang Y (2018) An Overview of Biomembrane Functions in Plant Responses to High-
634 Temperature Stress. *Frontiers in Plant Science* 9: 915

635 O'Sullivan O, Heskel M, Reich P, Tjoelker M, Weerasinghe L, Penillard A, Zhu L, Egerton J,
636 Bloomfield K, Creek D, Bahar N, Griffin K, Hurry V, Meir P, Turnbull M, Atkin O (2017)
637 Thermal limits of leaf metabolism across biomes. *Global Change Biology* 23(1): 209–
638 223

639 Pepin NC, Arnone E, Gobiet A, Haslinger K, Kotlarski S, Notarnicola C, Palazzi E, Seibert P,
640 Serafin S, Schöner W, Terzago S, Thornton JM, Vuille M, Adler C (2022) Climate
641 changes and their elevational patterns in the mountains of the world. *Reviews of*
642 *Geophysics* 60(1)

643 Perez TM, Feeley KJ (2020) Photosynthetic heat tolerances and extreme leaf temperatures.
644 *Functional Ecology* 34(11): 2236–2245

645 PlantNET (2024) (The NSW Plant Information Network System). Royal Botanic Gardens and
646 Domain Trust, Sydney

647 Posch BC, Hammer J, Atkin OK, Bramley H, Ruan Y-L, Trethowan R, Coast O (2022) Wheat
648 photosystem II heat tolerance responds dynamically to short- and long-term
649 warming. *Journal of Experimental Botany* 73(10): 3268–3282

650 R Development Core Team (2024) R: A language and environment for statistical computing.
651 R Foundation for Statistical Computing, Vienna, Austria

652 Rahnama A, Salehi F, Meskarbashee M, Mehdi Khanlou K, Ghorbanpour M, Harrison MT
653 (2024) High temperature perturbs physicochemical parameters and fatty acids
654 composition of safflower (*Carthamus tinctorius* L.). *BMC Plant Biology* 24(1): 1080

655 Roces V, Lamelas L, Valledor L, Carbó M, Cañal MJ, Meijón M (2022) Integrative analysis in
656 Pinus revealed long-term heat stress splicing memory. *The Plant Journal* 112(4): 998–
657 1013

658 Ru C, Hu X, Chen D, Wang W, Song T (2022) Heat and drought priming induce tolerance to
659 subsequent heat and drought stress by regulating leaf photosynthesis, root
660 morphology, and antioxidant defense in maize seedlings. *Environmental and
661 Experimental Botany* 202: 105010

662 Russell G, Marshall B, Jarvis PG (1989) Plant canopies: their growth, form and function.
663 Cambridge University Press, Cambridge & New York

664 Sastry A, Barua D (2017) Leaf thermotolerance in tropical trees from a seasonally dry climate
665 varies along the slow-fast resource acquisition spectrum. *Scientific Reports* 7(1):
666 11246

667 Seemann JR, Downton WJ, Berry JA (1986) Temperature and leaf osmotic potential as
668 factors in the acclimation of photosynthesis to high temperature in desert plants.
669 *Plant Physiology* 80(4): 926–930

670 Sklenář P, Kučerová A, Macková J, Romoleroux K (2016) Temperature microclimates of
671 plants in a tropical alpine environment: how much does growth form matter? *Arctic,
672 Antarctic, and Alpine Research* 48(1): 61–78

673 Song G, Wang Q (2023) Coupling effective variable selection with machine learning
674 techniques for better estimating leaf photosynthetic capacity in a tree species (*Fagus
675 crenata* Blume) from hyperspectral reflectance. *Agricultural and Forest Meteorology*
676 338: 109528

677 Sumner EE, Williamson VG, Gleadow RM, Wevill T, Venn SE (2022) Acclimation to water
678 stress improves tolerance to heat and freezing in a common alpine grass. *Oecologia*
679 199(4): 831–843

680 Valliere JM, Nelson KC, Martinez MC (2023) Functional traits and drought strategy predict
681 leaf thermal tolerance. *Conservation Physiology* 11(1): coad085

682 Vilas-Boas T, Almeida HAd, Della Torre F, Modolo LV, Lovato MB, Lemos-Filho JP (2024)
683 Intraspecific variation in the thermal safety margin in *Coffea arabica* L. in response to
684 leaf age, temperature, and water status. *Scientia Horticulturae* 337: 113455

685 Wahid A, Gelani S, Ashraf M, Foolad MR (2007) Heat tolerance in plants: An overview.
686 *Environmental and Experimental Botany* 61(3): 199–223

687 Wang W, Vinocur B, Altman A (2003) Plant responses to drought, salinity and extreme
688 temperatures: towards genetic engineering for stress tolerance. *Planta* 218(1): 1–14

689 Willits DH, Peet MM (1998) The effect of night temperature on greenhouse grown tomato
690 yields in warm climates. *Agricultural and Forest Meteorology* 92(3): 191–202

691 Yadav R, Juneja S, Kumar R, Saini R, Kumar S (2022) Understanding cross-tolerance
692 mechanism and effect of drought priming on individual heat stress and
693 combinatorial heat and drought stress in chickpea. *Journal of Crop Science and
694 Biotechnology* 25(5): 515–533

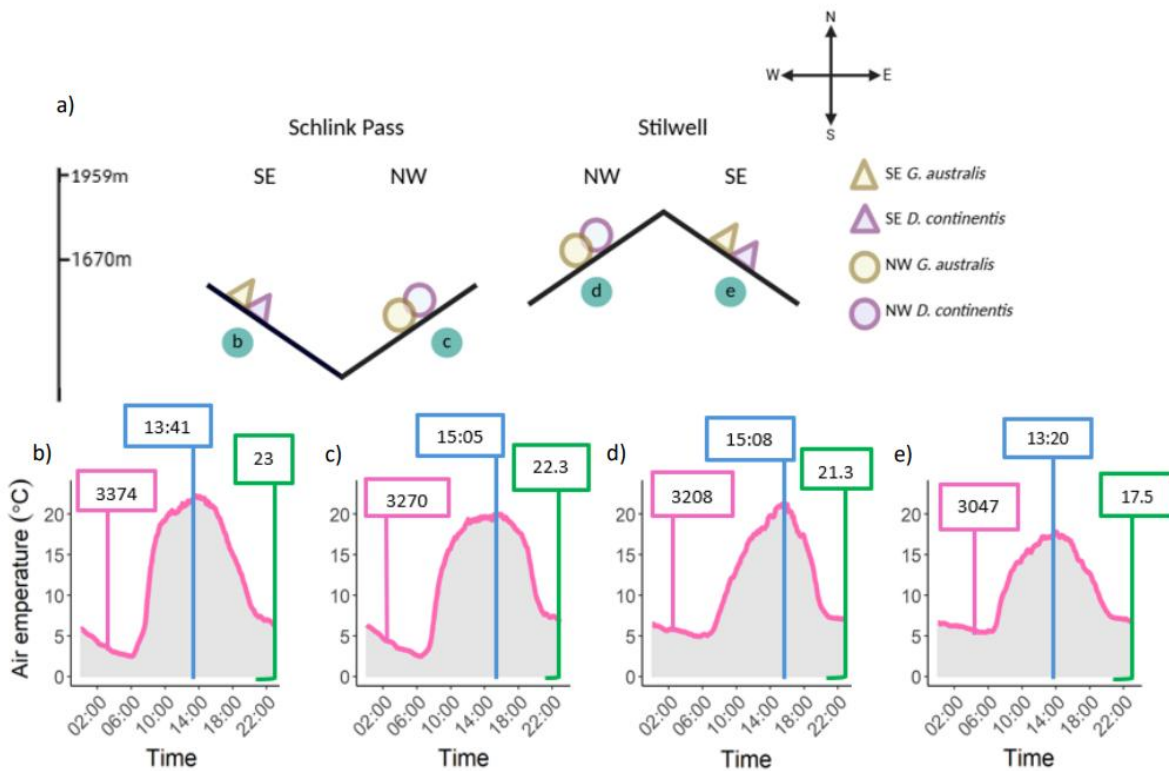
695 Yang Z, Tian J, Wang Z, Feng K (2022) Monitoring the photosynthetic performance of grape
696 leaves using a hyperspectral-based machine learning model. European Journal of
697 Agronomy 140: 126589

698 Zhang X, Rademacher T, Liu H, Wang L, Manzanedo RD (2023) Fading regulation of diurnal
699 temperature ranges on drought-induced growth loss for drought-tolerant tree
700 species. Nature Communications 14(1): 6916

701 Zhu L, Scafaro A, Vierling E, Ball M, Posch B, Stock F, Atkin O (2024) Heat tolerance of a
702 tropical–subtropical rainforest tree species *Polyscias elegans*: time-dependent
703 dynamic responses of physiological thermostability and biochemistry. New
704 Phytologist 241(2): 715–731

705 Zhu L, Bloomfield KJ, Hocart CH, Egerton JJ, O'Sullivan OS, Penillard A, Weerasinghe LK, Atkin
706 OK (2018) Plasticity of photosynthetic heat tolerance in plants adapted to thermally
707 contrasting biomes. Plant, Cell & Environment 41(6): 1251–1262

708

709 **Figure legends**

710

711 Figure 1. A schematic of the experimental design capturing microclimatic variation. a) site
 712 and aspect contrasts; both species (*Grevillea australis* and *Dracophyllum continentis*) at
 713 study sites contrasting in aspect throughout Schlink Pass and Mt Stilwell. The average
 714 elevation of sites at each location can be seen on the left. Black letters in green circles
 715 correspond with a site type, the air temperature parameters of which are indicated in panels
 716 b, c, d and e. T_{sum}^{air} (°C) represents the daily average sum of degrees above 0°C occurring at
 717 5-minute intervals across a 24-hr period (pink boxes, left); T_{time}^{air} represents the time of day
 718 at which maximum air temperatures occurred (blue boxes, middle) and T_{range}^{air} (°C)
 719 represents the diurnal range of air temperature (green boxes, right). Daily values for all three
 720 parameters were averaged across the month of February 2023 and across the four replicates
 721 of each site type (SchlinkSE, SchlinkNW, StilwellNW and StilwellSE). For full details, see
 722 Tables S1 and S2.

723

724 Table 1. The output of linear mixed models to determine the influence of aspect (NW v SE)
 725 and location (Schlink Pass v Mt Stilwell) on site-specific daily heat sum ($T_{\text{sum}}^{\text{air}}$), time of day
 726 that maximum temperatures were reached ($T_{\text{time}}^{\text{air}}$) and diurnal temperature range ($T_{\text{range}}^{\text{air}}$)
 727 across the month of February 2023. The model included the sampling date as a random
 728 factor to account for variation in heat sum caused by differences in weather across days
 729 (Figure S5). Bolded p-values indicate significance at $\alpha = 0.05$.

Response variable	df	Fixed effects	F	p-value
$T_{\text{time}}^{\text{air}}$	1, 415	Aspect	29.66	<0.001
	1, 415	Location	0.293	0.589
	1, 415	Aspect x location	0.490	0.484
$T_{\text{sum}}^{\text{air}}$	1, 415	Aspect	0.225	0.636
	1, 415	Location	10.467	0.001
	1, 415	Aspect x location	4.971	0.026
$T_{\text{range}}^{\text{air}}$	1, 425	Aspect	0.180	0.666
	1, 425	Location	24.79	<0.001
	1, 425	Aspect x location	22.12	<0.001

730

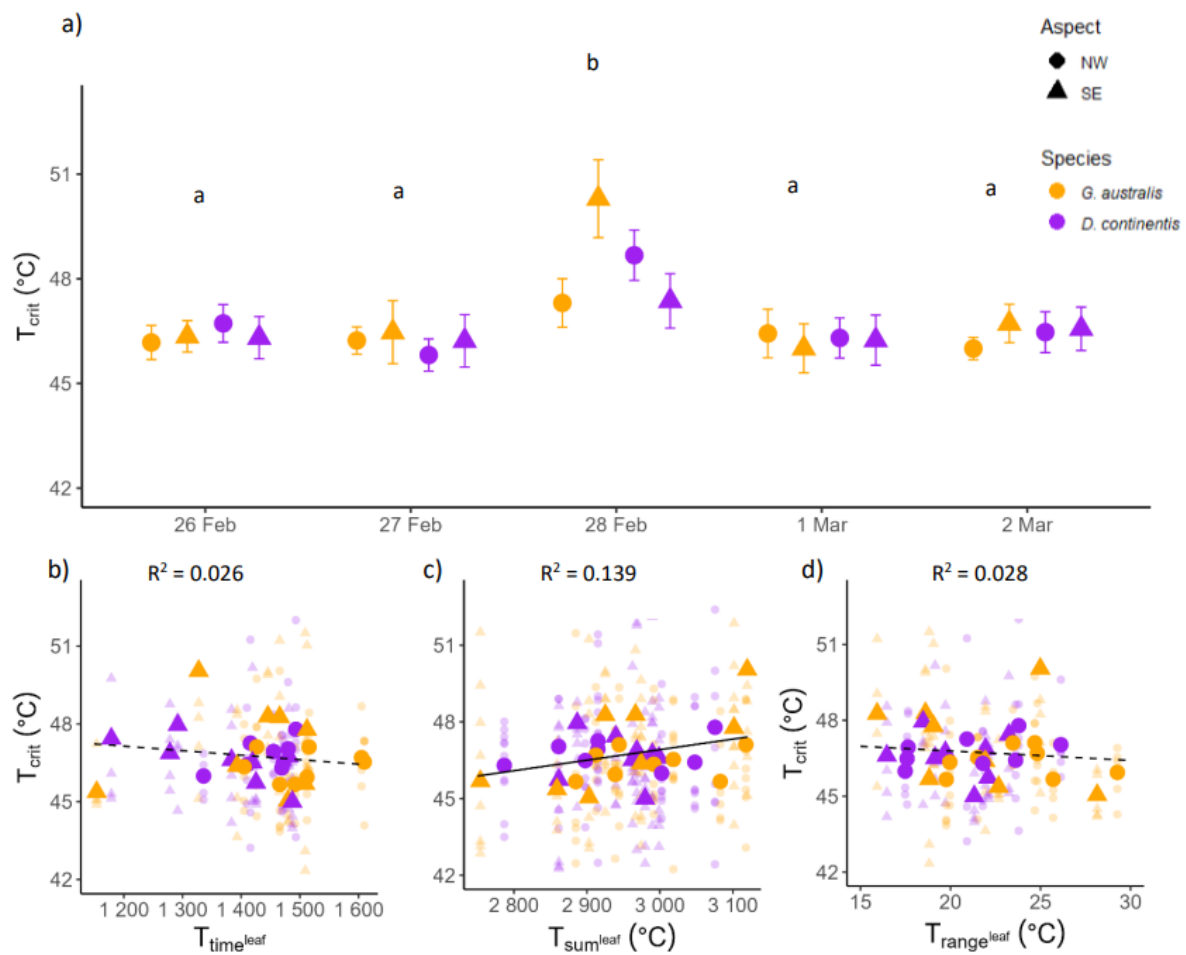
731 Table 2. The output of linear mixed models to determine the effect of leaf temperature
 732 parameters ($T_{\text{time}}^{\text{leaf}}$, $T_{\text{sum}}^{\text{leaf}}$, and $T_{\text{range}}^{\text{leaf}}$; Figure 2) on photosystem heat thresholds (T_{crit}).
 733 Bolded p-values indicate significance at $\alpha = 0.05$.

Leaf temperature parameter	df	F	p-value
$T_{\text{time}}^{\text{leaf}}$	1, 33	0.129	0.72
$T_{\text{sum}}^{\text{leaf}}$	1, 27	4.478	0.04
$T_{\text{range}}^{\text{leaf}}$	1, 20	0.527	0.47

734

735

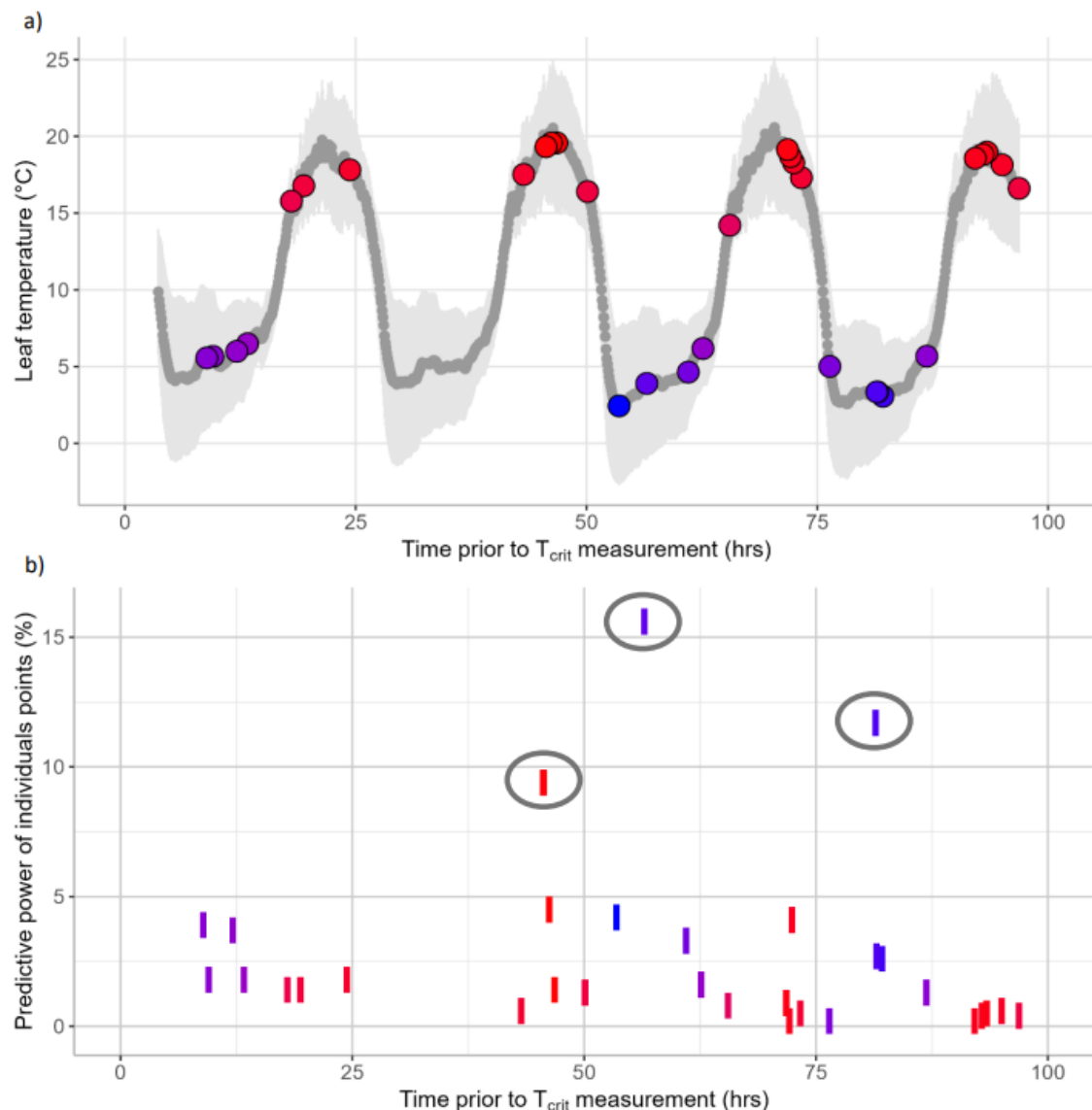
736 Figure 2. a) Variation in heat tolerance thresholds (T_{crit}) across five days of sampling in
 737 summer (26 Feb – 2 Mar). Letters represent significant differences in T_{crit} between days of
 738 sampling. Error bars show the standard error of mean T_{crit} . All daily T^{leaf} parameter values
 739 were averaged across the week of leaf temperatures leading up to and coinciding with T_{crit}
 740 sampling (22 Feb – 28 Feb). b) The relationship between average time of maximum
 741 temperature (T_{time}^{leaf}) and T_{crit} . c) The relationship between average daily heat sum (T_{sum}^{leaf})
 742 and T_{crit} . d) The relationship between average diurnal temperature range (T_{range}^{air}) and T_{crit} .
 743 Solid lines represent statistically significant relationships, and dashed lines represent non-
 744 significant relationships from linear mixed models; conditional R^2 values are shown above
 745 their corresponding relationship.



746

747

748 Figure 3. Snap Boosting Machine Regressor model for predicting the effects of the historical
 749 leaf temperature profiles on heat tolerance thresholds (T_{crit}) based on leaf temperatures
 750 averaged across two species and 16 sites recorded at 5-minute intervals (1,152 time points
 751 per day of T_{crit} measurement). The data shown represent the leaf temperature profile within
 752 the four days preceding each of the five days of T_{crit} measurement. Because T_{crit} was
 753 measured on five consecutive days, a given time point prior to T_{crit} measurement
 754 represented five sets of species-site combinations (32 plants per day totalling to 36,864 leaf
 755 temperatures for each day of T_{crit} measurement, Figure S6). (a) Leaf temperature (°C) over
 756 the four-days, with individual timepoints shown in dark grey and the light grey shadow
 757 indicating the standard deviation for each time point. Machine learning (ML) predictive
 758 features are the 33 points highlighted in colours representing their temperature, with blue
 759 indicating lower and red indicating higher leaf temperatures. The ML predictive points
 760 indicate the times at which leaf temperature had the highest predictive power for T_{crit}
 761 measured. (b) The individual predictive power of each of the 33 ML features, with the total
 762 predictive power of all points taken together explaining 84.9% of the variation in T_{crit} , with
 763 three temperature points having between 10-15% predictive power each (marked with grey
 764 ellipses).



765

1 *Supplementary Materials*

2 **Supporting Information 1.** Selection of sites contrasting in aspect.

3 Selection for each site pair was based on four criteria: 1) whether sites were reasonably
4 matched in elevation (within 10 m), 2) whether their aspects were contrasting (North-West
5 facing vs South-East facing), and 3) whether the distance between the target *G. australis*
6 and *D. continentis* plants was more than 1 m apart. The latter criterion was to ensure that
7 thermocouples were run only a short distance to the datalogger and that microclimatic
8 conditions that the plants were exposed to were comparable.

9
10
11

Table S1. Coordinates, elevation, slope and aspect of study microsites across Schlink Pass and Mt Stilwell in Kosciuszko National Park of South-East New South Wales. Latitude and longitude values are formatted in decimal degrees. The nomenclature of the site names are as follows: the first two letters, 'Sp' and 'St' represent the site location, Schlink Pass and Stilwell, respectively and the last two letters of each abbreviated site name represent the aspect of the site. Although not all sites were directly NW/SE facing, a LMM where date was a random factor revealed highly significant variation in mean air temperatures between sites of opposing aspects across the year 2023 ($p < 0.001$, Bird et al., unpublished data). This justified the grouping of paired sites into NW and SE categories.

Site	Latitude	Longitude	Elevation	Aspect	Slope
	(m a.s.l)				
Stilwell					
St1SE	-36.44111	148.3239	1962	SE 175 °	5 °
St1NW	-36.44111	148.3225	1953	NW 300 °	15 °
St2SE	-36.44778	148.3322	1959	SE 125 °	10 °
St2NW	-36.44222	148.3264	1960	NW 332 °	10 °
St3SE	-36.44583	148.3328	1952	SE 117 °	5 °
St3NW	-36.44194	148.3278	1963	NW 322 °	10 °
St4SE	-36.44472	148.3344	1956	NE 27 °	15 °
St4NW	-36.4428	148.3297	1963	NW 322 °	10 °
Schlink Pass					
Sp1SE	-36.26444	148.3731	1690	E 120 °	25 °
Sp1NW	-36.26477	148.3733	1680	NW 330 °	10 °
Sp2SE	-36.26694	148.3714	1672	E 70 °	20 °
Sp2NW	-36.26719	148.3719	1672	W 270 °	5 °
Sp3SE	-36.26806	148.3711	1667	E 90 °	20 °
Sp3NW	-36.26843	148.3718	1660	SW 240 °	15 °
Sp4SE	-36.26861	148.3708	1665	SE 150 °	5 °
Sp4NW	-36.26889	148.3708	1664	NW 300 °	5 °

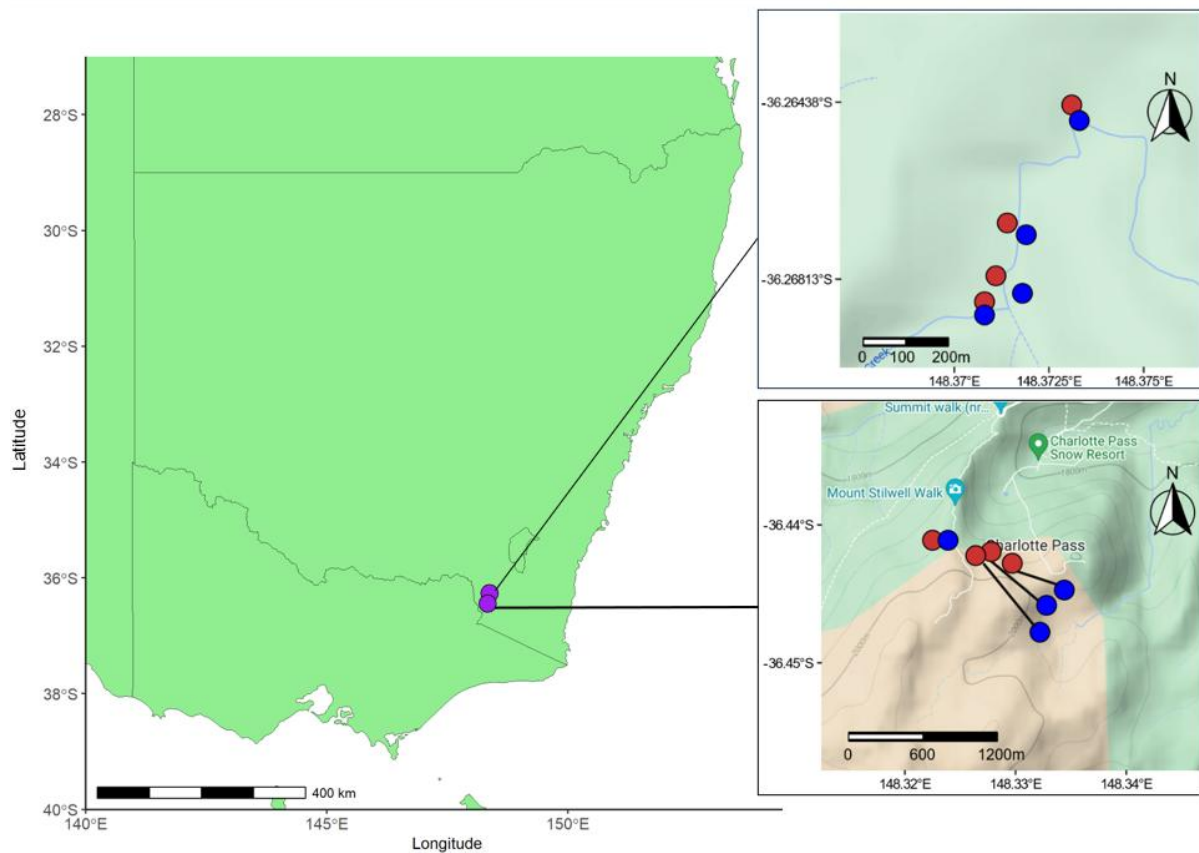


Figure S1: Sixteen study sites throughout Schlink Pass (top) and Mt Stilwell (bottom) in South-Eastern Australia on topographic maps. Red circles indicate N-NW facing sites; blue circles indicate S-SE facing sites. At each location, there were four site pairs, each pair matched in elevation but contrasted in aspect. Thin black lines indicate which sites are paired where unclear. Scale bars and north arrows are on each map. The map products were generated using the “*ggmap*” (Kahle & Wickham, 2013) and “*ggplot2*” (Wickham, 2016) R packages.

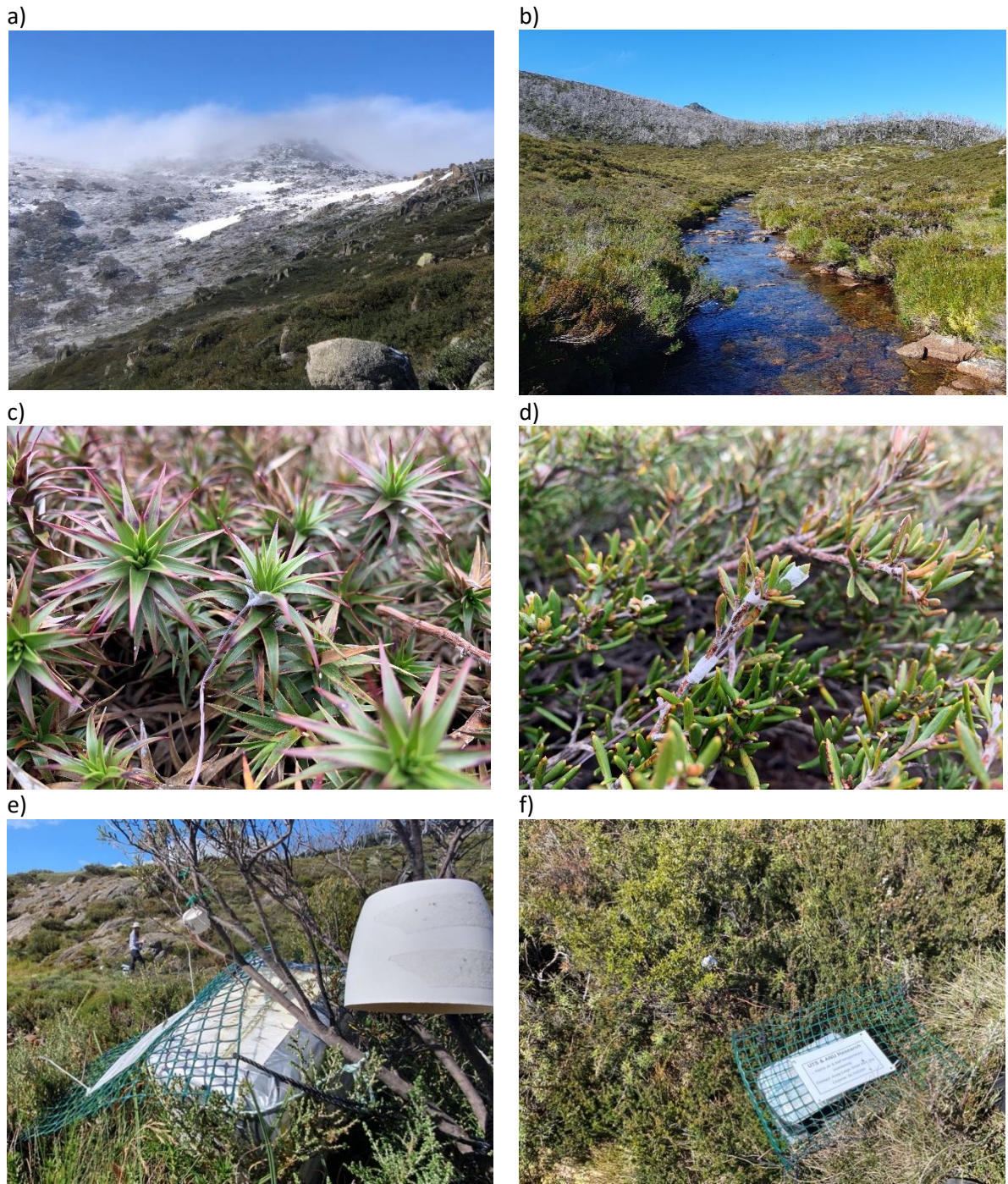


Figure S2. In-field setup of temperature logging stations at study microsites in Kosciuszko National Park, New South Wales across two locations: a) Mount Stilwell and b) Schlink Pass. Thermocouples recording leaf temperature of c) *D. continentis* and d) *G. australis*. e) A Thermocouple recording air temperature protected by a white cap. f) Thermocouples were connected to dataloggers and kept in a waterproof esky, protected using plastic garden netting.

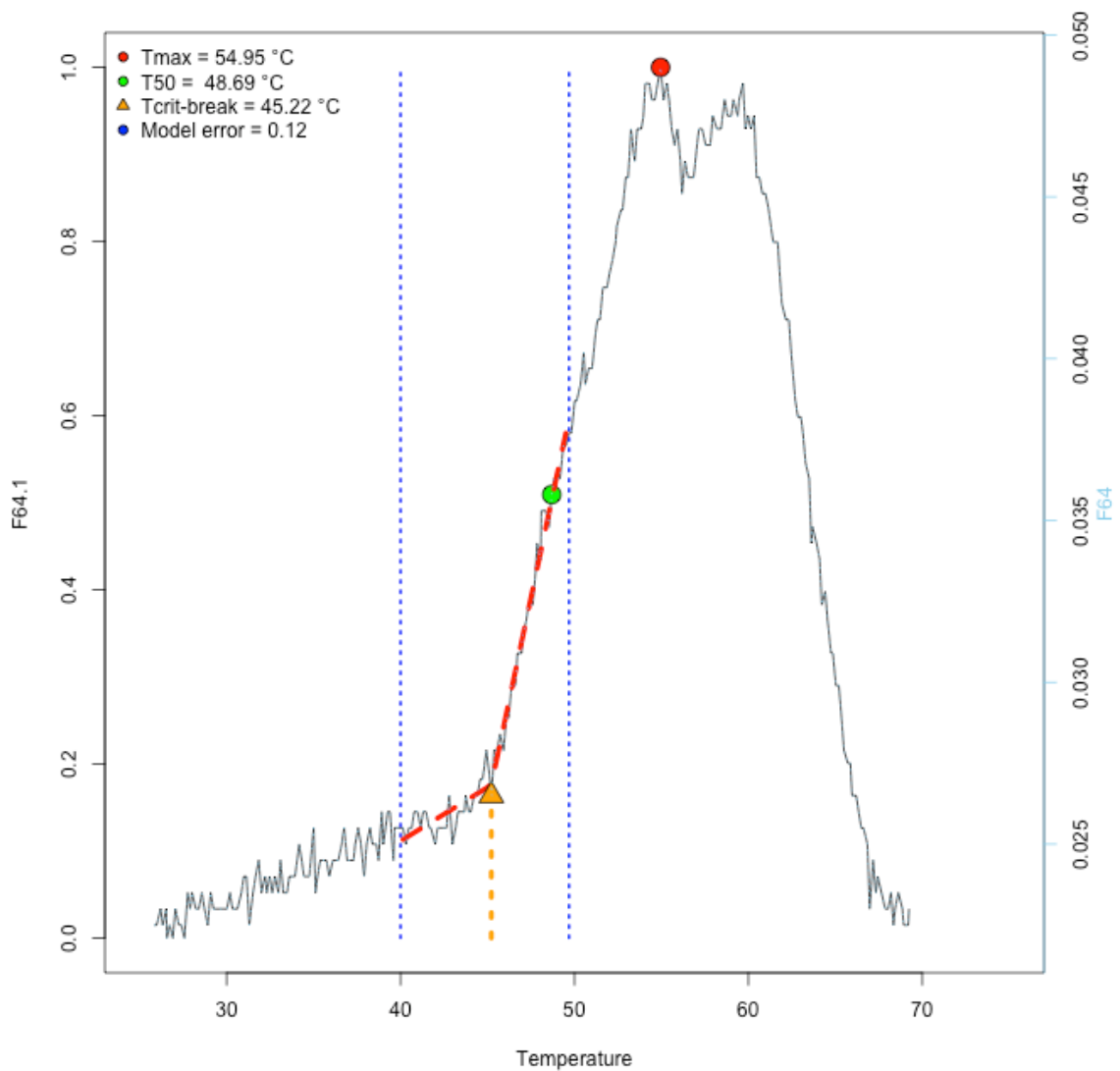


Figure S3. An example of a chlorophyll-fluorescence curve (T-F₀). The curve shows an increase in baseline chlorophyll fluorescence with an increase in temperature. The triangle indicates the T_{crit} threshold.

Table S2. Average maximum and minimum air temperatures, T_{time}^{air} , T_{sum}^{air} and T_{range}^{air} for NW and SE aspects at both study locations. Values for each variable were averaged across the four replicates for each site type and the 28 days of February 2023.

Location	Aspect	Mean maximum air temperature (°C)	Mean minimum air temperature (°C)	T_{time}^{air} (hrs)	T_{sum}^{air} (°C)	T_{range}^{air} (°C)
Schlink Pass	NW	22.5 ± 0.5	0.86 ± 0.3	15.1 ± 0.2	3269 ± 93	22.3 ± 0.7
	SE	24.9 ± 0.6	0.4 ± 0.3	13.7 ± 0.2	3373 ± 101	23.0 ± 0.6
Mt Stilwell	NW	24.3 ± 0.8	3.1 ± 0.3	15.1 ± 0.4	3208 ± 108	21.3 ± 0.8
	SE	20.6 ± 0.9	3.1 ± 0.3	13.3 ± 0.4	3047 ± 128	17.5 ± 0.9

20

Table S3. The output of linear mixed models to determine the influence of aspect (NW v SE) and location (Schlink Pass v Mt Stilwell) on site-specific daily heat sum (T_{sum}^{air}), time of day that maximum temperatures were reached (T_{time}^{air}) and diurnal temperature range (T_{range}^{air}) across the month of February 2023. The model included the sampling date as a random factor to account for variation in heat sum caused by differences in weather across days (Figure S5). Bolded p-values indicate significance at $\alpha = 0.05$.

Response variable	df	Explanatory variables	F	p-value
T_{time}^{air}	1, 415	Aspect	29.66	<0.001
	1, 415	Location	0.293	0.589
	1, 415	Aspect x location	0.490	0.484
T_{sum}^{air}	1, 415	Aspect	0.225	0.636
	1, 415	Location	10.467	0.001
	1, 415	Aspect x location	4.971	0.026
T_{range}^{air}	1, 425	Aspect	0.180	0.666
	1, 425	Location	24.79	<0.001
	1, 425	Aspect x location	22.12	<0.001

21

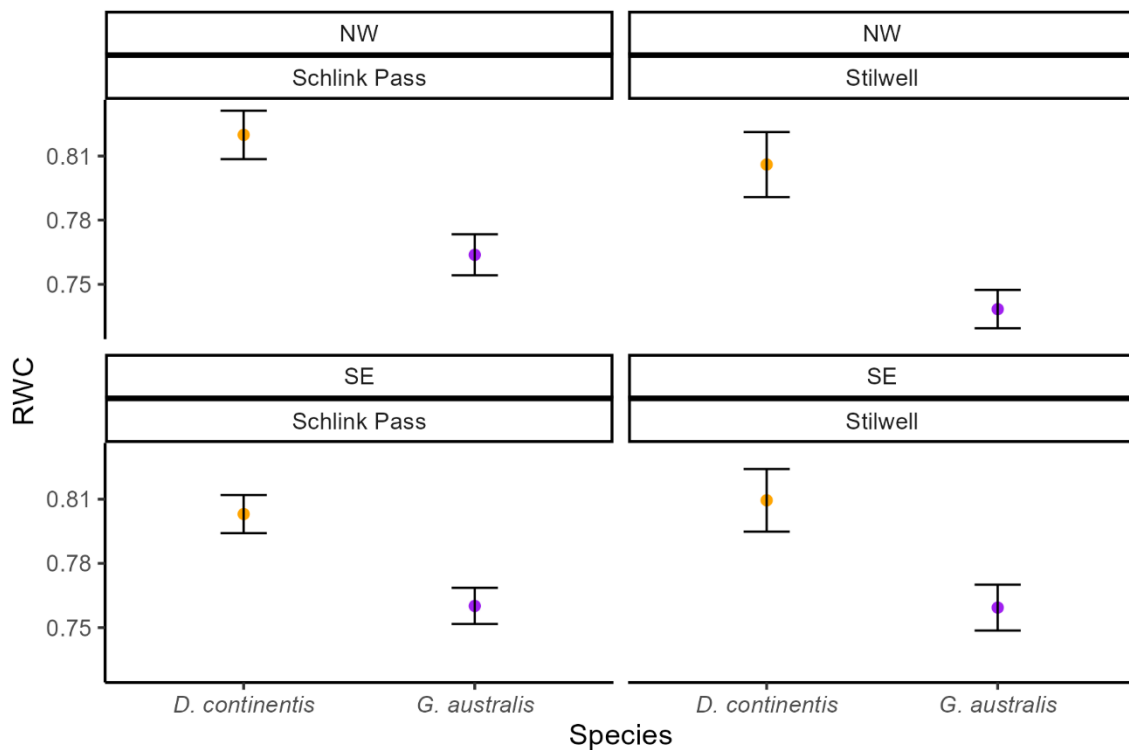
Table S4. The output of linear mixed models to determine the effect of leaf temperature parameters ($T_{\text{sum-day}}^{\text{leaf}}$, and $T_{\text{sum-night}}^{\text{leaf}}$; Figure 2) on photosystem heat thresholds (T_{crit}).

Leaf temperature parameter	df	F	p-value
$T_{\text{sum-day}}^{\text{leaf}}$	1, 27	3.07	0.99
$T_{\text{sum-night}}^{\text{leaf}}$	1, 27	3.1	0.09

22

23

Figure S4. RWC for *G. australis* and *D. continentis* at the four site-types (SchlinkSE, SchlinkNW, StilwellNW, StilwellSE). All data were collected between the 25 Feb and 1 March 2023, overlapping with the T_{crit} sampling period.



24

25

26

27

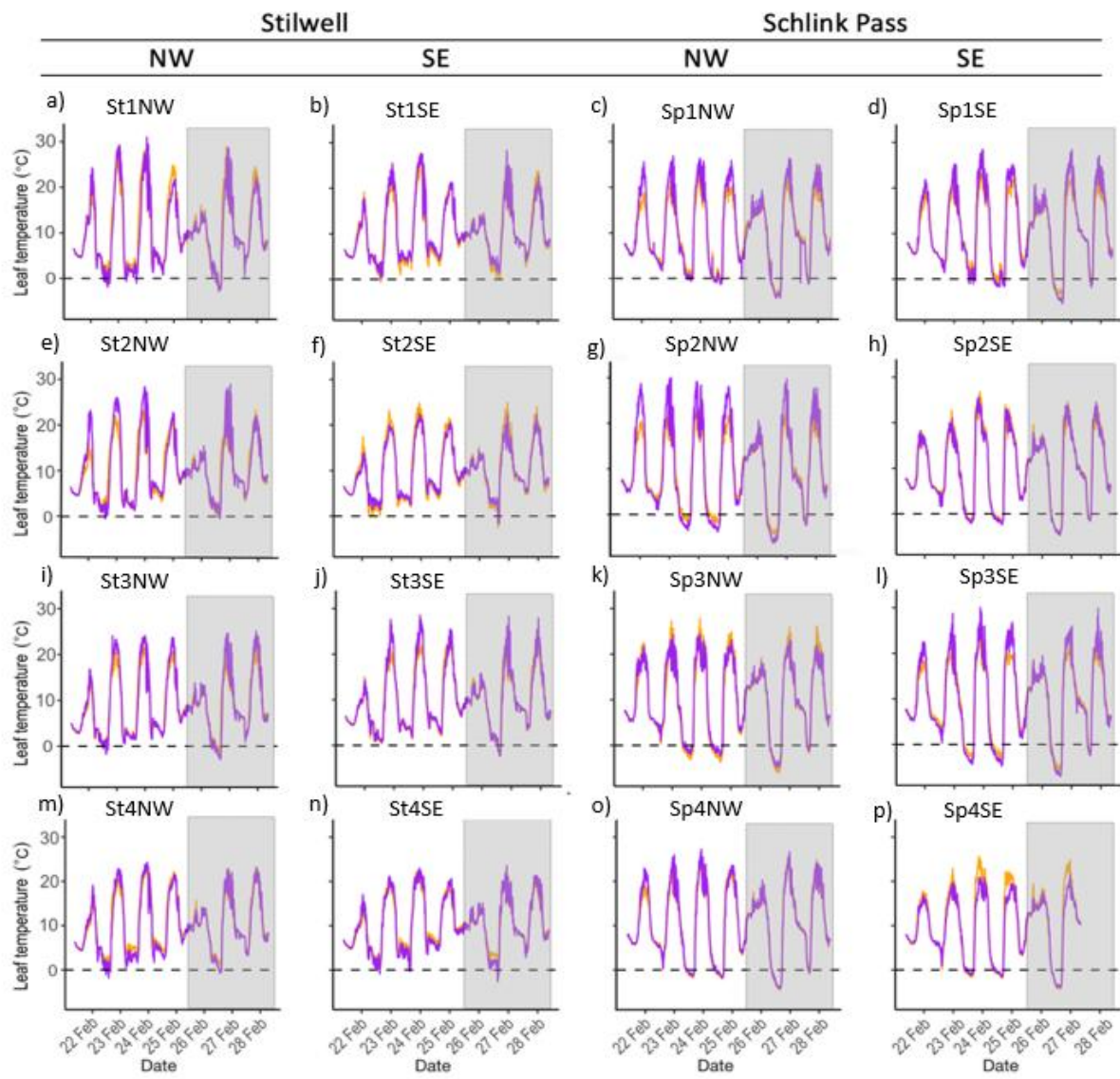


Figure S5. Leaf temperatures ($^{\circ}\text{C}$) of *Dracophyllum continentis* (purple lines) and *Grevillea australis* (yellow lines) across seven days (22–28 Feb) leading up to and coinciding with T_{crit} sampling (26 Feb–2 Mar). Leaf temperatures were measured in situ at 16 sites across two alpine locations (Schlink Pass and Mt Stilwell) that contrasted in aspect (SW v NE). Tick marks on the x-axis align with data recorded at 3 pm on that day. The dashed horizontal lines represent 0°C , and the grey shading represents the first three days of T_{crit} sampling.

22 Feb	23 Feb	24 Feb	25 Feb	26 Feb	28 Feb	1 Mar	2 Mar	Time points	Leaf temperature points
			T_{crit}	T_{crit}	T_{crit}	T_{crit}	T_{crit}		
288	288	288	288					1152	36864
	288	288	288	288				1152	36864
		288	288	288	288			1152	36864
			288	288	288	288		1152	36864
				288	288	288	288	1152	36864
288	576	864	1552	1152	864	576	288	5760	184320

Figure S6. Number of time points and leaf temperatures included in the SnapBoosting Machine Regressor model used to predict the effects of historical leaf temperature profiles on heat tolerance thresholds (T_{crit}). Time points for each four-day period preceding a day of T_{crit} measurements are shown in rows 3–7. The darkest shade represents time points within the 24 hours preceding each day of T_{crit} measurement, while the lightest shade represents time points 72–96 hours prior. Each time point corresponds to 32 unique leaf temperature measurements (recorded from two species across 16 sites). In total, 1,552 time points and 36,864 unique leaf temperature values were used to predict the 32 T_{crit} values for each measurement day. Across all 32 plants and all five T_{crit} measurement days, a total of 5,670 time points and 184,320 leaf temperature values were used to predict T_{crit} in this four-day model.

34
35
36
37
38

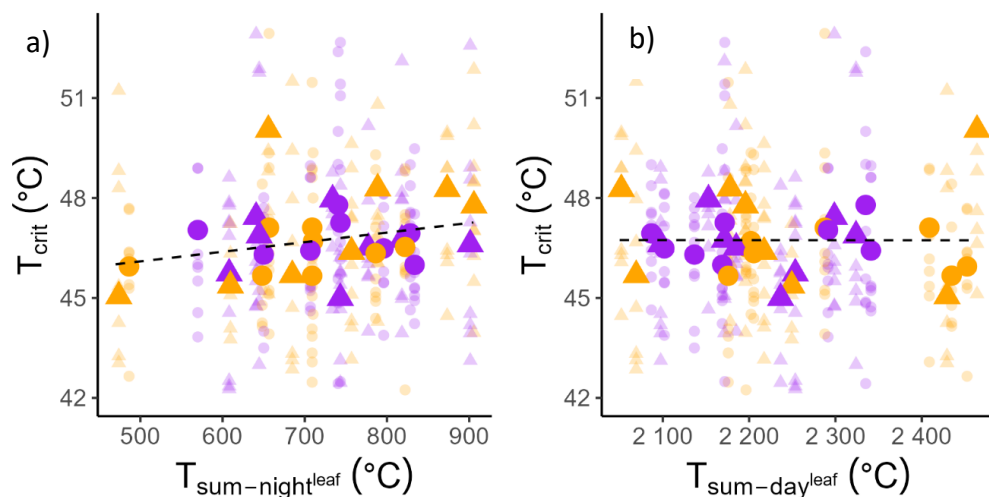


Figure S7. Daily T^{leaf} parameters values were averaged across the week of leaf temperatures leading up to and coinciding with T_{crit} sampling (22 Feb – 28 Feb). a) The relationship between average day time heat sum ($T_{\text{sum-night}}^{\text{leaf}}$) and T_{crit} . b) The relationship between average day time heat sum ($T_{\text{sum-night}}^{\text{leaf}}$) and T_{crit} . Dashed lines represent non-significant relationships from linear mixed models.

39
40
41

42 Bird, M., Pottinger, C., Arnold, P., Danzey, L., Geange, S., Kearney, M., . . . Leigh, A.
43 (unpublished data). Can NicheMapR predict leaf temperatures of morphologically
44 disparate species across microclimatically distinct alpine sites?
45 Kahle, D., & Wickham, H. (2013). ggmap: Spatial Visualization with ggplot2. *The R Journal*,
46 5(1), 144-161.
47 Leon-Garcia, I. V., & Lasso, E. (2019). High heat tolerance in plants from the Andean
48 highlands: Implications for paramos in a warmer world. *PLoS One*, 14(11), e0224218.
49 doi:10.1371/journal.pone.0224218
50 Wickham, H. (2016). *ggplot2: Elegant Graphics for Data Analysis*: Springer-Verlag New
51 York.
52
53
54